One-loop correction to the enhanced curvature perturbation with local-type non-Gaussianity for the formation of primordial black holes

De-Shuang Meng,[1,2,‡] Chen Yuan,[1,2,*] and Qing-Guo Huang[1,2,3,†]

[1]*CAS Key Laboratory of Theoretical Physics, Institute of Theoretical Physics, Chinese Academy of Sciences, Beijing 100190, China*

[2]*School of Physical Sciences, University of Chinese Academy of Sciences, No. 19A Yuquan Road, Beijing 100049, China*

[3]*School of Fundamental Physics and Mathematical Sciences Hangzhou Institute for Advanced Study, UCAS, Hangzhou 310024, China*

(Received 21 July 2022; accepted 30 August 2022; published 8 September 2022)

As one of the promising candidates of cold dark matter, primordial black holes (PBHs) were formed due to the collapse of overdense regions generated by the enhanced curvature perturbations during the radiation-dominated era. The enhanced curvature perturbations are expected to be non-Gaussian in some relevant inflation models, and hence, the higher-order loop corrections to the curvature power spectrum might be non-negligible as well as altering the abundance of PBHs. In this paper, we calculate the one-loop correction to the curvature power spectrum with local-type non-Gaussianities characterized by $F_{\rm NL}$ and $G_{\rm NL}$ standing for the quadratic and cubic non-Gaussian parameters, respectively. Requiring that the one-loop correction be subdominant, we find a perturbativity condition, namely, $|2cAF_{\rm NL}^2 + 6AG_{\rm NL}| \ll 1$, where c is a constant coefficient which can be explicitly calculated in the given model, and A denotes the variance of the Gaussian part of the enhanced curvature perturbation, and such a perturbativity condition can provide a stringent constraint on the relevant inflation models for the formation of PBHs.

DOI: 10.1103/PhysRevD.106.063508

I. INTRODUCTION

Primordial black holes (PBHs) can form from the collapse of overdense regions when large curvature perturbations reenter the horizon during the radiation-dominated era [1–4]. PBHs not only represent cold dark matter (DM) but also explain the merger events detected by the LIGO-Virgo Collaboration [5–15]. There are various investigations [6,15–40] putting constraints on the fraction of PBHs in DM to no more than a few percent except two mass windows $[10^{-16}, 10^{-14}]\ M_\odot \cup [10^{-13}, 10^{-12}]\ M_\odot$ [41,42]. Reviews of the constraints on PBHs can be found in [43,44].

It is estimated that the curvature power spectrum needs to be enhanced to about 10^{-2} in order to form sufficient PBHs on certain small scales, compared to those on the cosmic microwave background (CMB) scales, which is of order 10^{-9} [45]. PBHs are formed at the tail of the probability density function (PDF) of the curvature perturbations, and the tail is very sensitive to non-Gaussianity, which is very important to determine the abundance of PBHs [46–54]. On the other hand, in the squeezed limit of the bispectrum for canonical single-field inflation models, the Maldacena consistency condition [55] for the non-Gaussian parameter $f_{\rm NL}^{\rm sq}$ and the spectral index n_s, namely, $f_{\rm NL}^{\rm sq} = -5(n_s - 1)/12$, is usually expected to hold. Although this condition is violated in the ultra slow-roll model, there is still large local non-Gaussianity with $f_{\rm NL} = 5/2$ [56]. Therefore, non-negligible non-Gaussianities are usually accompanied by the enhancement of a power spectrum where the spectral index would be much larger, rendering non-Gaussianities that might play a significant role in those inflation models that predict large numbers of PBHs.

From the viewpoint of quantum field theory (QFT), if one takes the interaction picture, the power spectrum of curvature perturbations is equivalent to calculating the vacuum expectation value of a two-point correlation function (2PCF) and the non-Gaussianities correspond to an N-point correlation function (NPCF) with $N > 2$ by in-in formalism. On the other hand, the NPCF can make a contribution to the 2PCF through loop corrections. Based on the fact that loop corrections of a 2PCF need to be smaller than the tree level in order to maintain the significance of perturbation theory, the authors in [57] found a perturbativity condition such that $c_s^{-4}\mathcal{P}_\zeta \ll 1 - n_s$ for a single-field inflation model, where c_s represents the

*Corresponding author.
yuanchen@itp.ac.cn
†Corresponding author.
huangqg@itp.ac.cn
‡mengdeshuang@itp.ac.cn

sound speed, $\mathcal{P}_\zeta$ denotes the amplitude of the tree-level power spectrum, and $n_s < 1$ is the spectral index.

In this paper, we calculate the one-loop correction to the curvature power spectrum with local-type non-Gaussianities and work out the perturbativity condition for the enhanced curvature perturbation for the formation of PBHs. In addition to the constraints from loop corrections, the abundance of PBHs would naturally select the non-Gaussian parameters (see, e.g., [58]). We then investigate the constraints on non-Gaussian parameters by taking into account both the perturbativity condition and the PBH abundance. The paper is organized as follows. In Sec. II, we calculate the one-loop correction for the enhanced power spectra of curvature perturbations from local-type non-Gaussianities and work out the perturbativity condition. In Sec. III, we review the calculation of PBH abundance and obtain the constraints on the non-Gaussian parameters. Finally, we give a brief conclusion and discussion in Sec. IV.

II. CONSTRAINTS ON THE LOCAL-TYPE NON-GAUSSIAN PARAMETERS FROM ONE-LOOP CORRECTIONS

For the local-type non-Gaussianities, the curvature perturbation is expanded in terms of the Gaussian part in real space. Up to cubic order, it is given by

$$\zeta(\boldsymbol{x}) = \zeta_{\rm g}(\boldsymbol{x}) + F_{\rm NL}\zeta_{\rm g}^2(\boldsymbol{x}) + G_{\rm NL}\zeta_{\rm g}^3(\boldsymbol{x}), \tag{1}$$

where $\zeta_{\rm g}(\boldsymbol{x})$ follows Gaussian statistics, and $F_{\rm NL}$ and $G_{\rm NL}$ are the dimensionless non-Gaussian parameters related to the commonly used notations $f_{\rm NL}$ and $g_{\rm NL}$ by $F_{\rm NL} \equiv 3/5 f_{\rm NL}$ and $G_{\rm NL} \equiv 9/25 g_{\rm NL}$, respectively. In momentum space, the curvature perturbation is expanded by convolution of the Gaussian part

$$\zeta(\boldsymbol{k}) = \zeta_{\rm g}(\boldsymbol{k}) + F_{\rm NL}\int \frac{{\rm d}^3p}{(2\pi)^3}\zeta_{\rm g}(\boldsymbol{p})\zeta_{\rm g}(\boldsymbol{k}-\boldsymbol{p}) + G_{\rm NL}\int \frac{{\rm d}^3p}{(2\pi)^3}\int \frac{{\rm d}^3q}{(2\pi)^3}\zeta_{\rm g}(\boldsymbol{p})\zeta_{\rm g}(\boldsymbol{q})\zeta_{\rm g}(\boldsymbol{k}-\boldsymbol{p}-\boldsymbol{q}). \tag{2}$$

The dimensionless power spectrum of curvature perturbation $\mathcal{P}_\zeta(k)$ is defined as

$$\langle\zeta(\boldsymbol{k})\zeta(\boldsymbol{k}')\rangle = \frac{2\pi^2}{k^3}\mathcal{P}_\zeta(k)(2\pi)^3\delta^{(3)}(\boldsymbol{k}+\boldsymbol{k}'). \tag{3}$$

The one-loop correction from the local-type non-Gaussianities can be derived by inserting Eq. (2) into Eq. (3). According to the property of a Gaussian variable, the odd n-point functions vanish, the even n-point functions can be expanded by all possible contractions of the 2PCFs $\langle\zeta_{\rm g}(\boldsymbol{k})\zeta_{\rm g}(\boldsymbol{k}')\rangle$, and the final result can be expressed as

$$\begin{aligned}\langle\zeta(\boldsymbol{k})\zeta(\boldsymbol{k}')\rangle &= \langle\zeta_{\rm g}(\boldsymbol{k})\zeta_{\rm g}(\boldsymbol{k}')\rangle + \int \frac{{\rm d}^3p}{(2\pi)^3}\int \frac{{\rm d}^3q}{(2\pi)^3}[F_{\rm NL}^2\langle\zeta_{\rm g}(\boldsymbol{p})\zeta_{\rm g}(\boldsymbol{k}-\boldsymbol{p})\zeta_{\rm g}(\boldsymbol{q})\zeta_{\rm g}(\boldsymbol{k}'-\boldsymbol{q})\rangle \\ &\quad + 2G_{\rm NL}\langle\zeta_{\rm g}(\boldsymbol{k})\zeta_{\rm g}(\boldsymbol{p})\zeta_{\rm g}(\boldsymbol{q})\zeta_{\rm g}(\boldsymbol{k}'-\boldsymbol{p}-\boldsymbol{q})\rangle] \\ &= \langle\zeta_{\rm g}(\boldsymbol{k})\zeta_{\rm g}(\boldsymbol{k}')\rangle + \int \frac{{\rm d}^3p}{(2\pi)^3}\int \frac{{\rm d}^3q}{(2\pi)^3}[2F_{\rm NL}^2\langle\zeta_{\rm g}(\boldsymbol{p})\zeta_{\rm g}(\boldsymbol{q})\rangle\langle\zeta_{\rm g}(\boldsymbol{k}-\boldsymbol{p})\zeta_{\rm g}(\boldsymbol{k}'-\boldsymbol{q})\rangle \\ &\quad + 6G_{\rm NL}\langle\zeta_{\rm g}(\boldsymbol{k})\zeta_{\rm g}(\boldsymbol{p})\rangle\langle\zeta_{\rm g}(\boldsymbol{q})\zeta_{\rm g}(\boldsymbol{k}'-\boldsymbol{p}-\boldsymbol{q})\rangle],\end{aligned} \tag{4}$$

where the disconnected diagrams do not show up in the final physical process since they factor out as in the standard QFT process. Therefore, the dimensionless power spectrum can be written as

$$\mathcal{P}_\zeta(k) = \mathcal{P}_\zeta^{(0)}(k) + \mathcal{P}_\zeta^{(1)}(k), \tag{5}$$

where $\mathcal{P}_\zeta^{(0)}(k)$ is the Gaussian-part spectrum, and

$$\mathcal{P}_\zeta^{(1)}(k) = \frac{k^3F_{\rm NL}^2}{2\pi}\int {\rm d}^3p\,\frac{\mathcal{P}_\zeta^{(0)}(p)\mathcal{P}_\zeta^{(0)}(|\boldsymbol{k}-\boldsymbol{p}|)}{p^3|\boldsymbol{k}-\boldsymbol{p}|^3} + \frac{3G_{\rm NL}}{2\pi}\mathcal{P}_\zeta^{(0)}(k)\int {\rm d}^3p\,\frac{\mathcal{P}_\zeta^{(0)}(p)}{p^3} \tag{6}$$

is the one-loop correction. By introducing two variables $u = p/k$ and $v = |\boldsymbol{k}-\boldsymbol{p}|/k$, the one-loop correction can be rewritten as

$$\begin{aligned}\mathcal{P}_\zeta^{(1)}(k) &= F_{\rm NL}^2\int_0^\infty {\rm d}u\int_{|1-u|}^{1+u}{\rm d}v\,\frac{\mathcal{P}_\zeta^{(0)}(uk)\mathcal{P}_\zeta^{(0)}(vk)}{u^2v^2} + 6G_{\rm NL}\mathcal{P}_\zeta^{(0)}(k)\int {\rm d}p\,\frac{\mathcal{P}_\zeta^{(0)}(p)}{p} \\ &= F_{\rm NL}^2\int_0^\infty {\rm d}u\int_{|1-u|}^{1+u}{\rm d}v\,\frac{\mathcal{P}_\zeta^{(0)}(uk)\mathcal{P}_\zeta^{(0)}(vk)}{u^2v^2} + 6AG_{\rm NL}\mathcal{P}_\zeta^{(0)}(k),\end{aligned} \tag{7}$$

where A stands for the variance of the Gaussian part of curvature perturbation spectrum $\mathcal{P}_\zeta^{(0)}(k)$, namely,

$$A = \int \mathcal{P}_\zeta^{(0)}(k) \mathrm{d}\ln k, \tag{8}$$

and the variance of the one-loop correction $\mathcal{P}_\zeta^{(1)}(k)$ reads

$$\begin{aligned}\sigma^{(1)} &= \int \mathcal{P}_\zeta^{(1)}(k) \mathrm{d}\ln k \\ &= F_{\mathrm{NL}}^2 \int \mathrm{d}\ln k \int_0^\infty \mathrm{d}u \int_{|1-u|}^{1+u} \mathrm{d}v \frac{\mathcal{P}_\zeta^{(0)}(uk)\mathcal{P}_\zeta^{(0)}(vk)}{u^2 v^2} \\ &\quad + 6A^2 G_{\mathrm{NL}} \\ &= 2cA^2 F_{\mathrm{NL}}^2 + 6A^2 G_{\mathrm{NL}},\end{aligned} \tag{9}$$

where c is a constant coefficient which can be explicitly calculated for the given enhanced curvature perturbation. Usually, c is expected to be $\mathcal{O}(1)$ for some typical PBH formation models.

From the viewpoint of QFT, F_{NL} and G_{NL} should be regarded as the coupling constants. In general, the shape of the power spectrum from one-loop correction should be different from that in tree-level order. Quantitatively, the variance of the one-loop correction $\sigma^{(1)}$ is supposed to be much smaller than that of the tree-level order $\sigma^{(0)} = A$ in order to ensure the expansion converges. Therefore, the perturbativity condition for the enhanced curvature perturbation with local-type non-Gaussianities reads

$$|2cAF_{\mathrm{NL}}^2 + 6AG_{\mathrm{NL}}| \ll 1. \tag{10}$$

Note that G_{NL} can be positive or negative.

In the following part of this section, we will consider two typical models that are enhanced at a certain scale over the CMB scale, namely, an infinite narrow spectrum and a log-normal-shaped spectrum. These two models are commonly used in studying the formation of PBHs (see, e.g., [40,59–62]). Suppose that an enhanced power spectrum has a cutoff at k_{max} (or decreases dramatically if $k > k_{\mathrm{max}}$), then according to Eq. (6), the one-loop power spectrum will have a cutoff at $2k_{\mathrm{max}}$ due to the conservation of momentum. This indicates that, for an enhanced power spectrum which has a cutoff wavelength, the one-loop power spectrum is integrable, and one does not need to perform regularization and renormalization which is different from the case discussed in [57] where the authors consider a scale-invariant power spectrum.

The infinite narrow spectrum peaked at k_* at the tree level; namely, the δ spectrum is parametrized as

$$\mathcal{P}_\zeta^{(0)}(k) = Ak_*\delta(k - k_*). \tag{11}$$

Then, the one-loop correction to the δ power spectrum for the local non-Gaussian expansion can be analytically expressed by

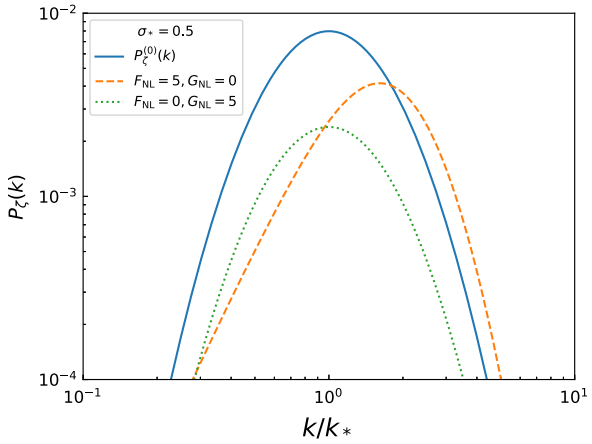

FIG. 1. The log-normal power spectrum (the blue solid line) and its one-loop corrections (dashed and dotted lines) of local-type non-Gaussianities with different F_{NL} and G_{NL}. The width of the Gaussian spectrum and its variance are fixed at $\sigma_* = 0.5$ and $A = 10^{-2}$, respectively.

$$\begin{aligned}\mathcal{P}_\zeta^{(1)}(k) &= A^2 F_{\mathrm{NL}}^2 \left(\frac{k}{k_*}\right)^2 \Theta\left(2 - \frac{k}{k_*}\right) \\ &\quad + 6A^2 G_{\mathrm{NL}} k_* \delta(k - k_*),\end{aligned} \tag{12}$$

and the variance of the one-loop correction is $\sigma^{(1)} = 2A^2F_{\mathrm{NL}}^2 + 6A^2G_{\mathrm{NL}}$ corresponding to $c = 1$ in Eq. (9).

The log-normal-shaped spectrum is given by

$$\mathcal{P}_\zeta^{(0)}(k) = \frac{A}{\sqrt{2\pi\sigma_*^2}} \exp\left(-\frac{\ln^2(k/k_*)}{2\sigma_*^2}\right), \tag{13}$$

where the dimensionless parameter σ_* is related to the width of the spectrum ($\sim e^{\sigma_*}$). The total one-loop correction is the sum of the contributions of the F_{NL} and G_{NL} terms and depends on the values of F_{NL} and G_{NL}. The G_{NL} term in one-loop correction only causes a constant shift $6AG_{\mathrm{NL}}$, while the F_{NL} term needs to be calculated numerically. The tree-level and one-loop power spectrum are shown in Fig. 1 for $F_{\mathrm{NL}} = 0$, $G_{\mathrm{NL}} = 5$ and $F_{\mathrm{NL}} = 5$, $G_{\mathrm{NL}} = 0$, where we set $A = 10^{-2}$ and $\sigma_* = 0.5$. For the log-normal power spectrum, the coefficient c in Eq. (9) depends on the width of the tree-level spectrum and is shown in Fig. 2. We see that the coefficient c is roughly smaller than $\mathcal{O}(1)$ despite the width.

III. CONSTRAINTS ON THE NON-GAUSSIAN PARAMETERS COMBINED WITH THE ABUNDANCE OF PBHs

In this section, we will briefly review the abundance of PBHs and give the constraints on the non-Gaussian parameters by considering both loop correction and the abundance of PBHs. Throughout this section, we will consider a δ-spectrum described by Eq. (11).

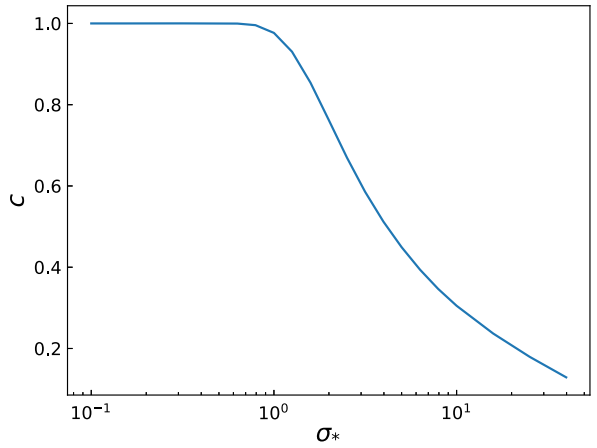

FIG. 2. The value of c as a function of the width of the log-normal spectrum σ_*.

Let $P(\zeta)$ to be the PDF of ζ, then the initial mass function of the PBHs β can be estimated by integrating the PDF over the region $\zeta > \zeta_c$ where $\zeta_c \sim \mathcal{O}(1)$ [63–66] is the critical value to form a single PBH:

$$\beta = \int_{\zeta>\zeta_c} P(\zeta)\mathrm{d}\zeta = \int_{\zeta(\zeta_g)>\zeta_c} \frac{1}{\sqrt{2\pi A}} \exp\left(-\frac{\zeta_g^2}{2A}\right)\mathrm{d}\zeta_g, \quad (14)$$

where we have used $\langle\zeta_g^2\rangle = \int \mathcal{P}_\zeta^{(0)}(k)\mathrm{d}\ln k = A$. Note that the proper quantity to compute the probability of forming PBHs is the volume average density contrast δ instead of ζ as shown in [67]. However, we aim to discuss the possibility to constrain non-Gaussianities using both loop corrections and PBHs rather than evaluating a precise upper (or lower) bound. Also, for a peaked power spectrum, we can use ζ approximately, and β is related to the fraction of PBH DM by [68]

$$f_{\mathrm{pbh}} \simeq 2.5 \times 10^8 \beta \left(\frac{g_*^{\mathrm{form}}}{10.75}\right)^{-\frac{1}{4}} \left(\frac{m_{\mathrm{pbh}}}{M_\odot}\right)^{-\frac{1}{2}}, \quad (15)$$

with g_*^{form} and m_{pbh} the effective degrees of freedom and the mass of PBHs at the formation time, respectively. A fixed f_{pbh} would select the values of A, F_{NL}, and G_{NL}. In the following part, we consider that all DM is in the form of $10^{-12}\ M_\odot$ PBHs, namely, $f_{\mathrm{pbh}} = 1$, and then $\beta \simeq 7 \times 10^{-15}$.

First of all, for a pure F_{NL} model where $G_{\mathrm{NL}} = 0$, the equation $\zeta(\zeta_g) = \zeta_c$ is solved as

$$\zeta_{g\pm} = \frac{-1 \pm \sqrt{1 + 4F_{\mathrm{NL}}\zeta_c}}{2F_{\mathrm{NL}}}. \quad (16)$$

If $F_{\mathrm{NL}} > 0$, β can be expressed as

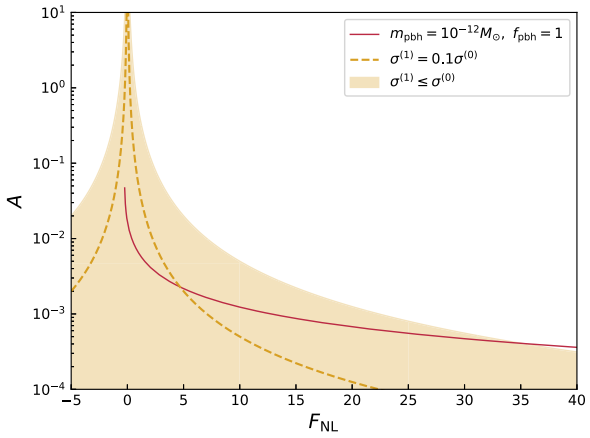

FIG. 3. The allowed parameter space for A and F_{NL} in the case of $G_{\mathrm{NL}} = 0$. The shaded region corresponds to $|\sigma^{(1)}/\sigma^{(0)}| \le 1$, and the dashed line corresponds to $|\sigma^{(1)}/\sigma^{(0)}| = 0.1$. The solid red line stands for $m_{\mathrm{pbh}} = 10^{-12}\ M_\odot$ and $f_{\mathrm{pbh}} = 1$.

$$\beta = \int_{-\infty}^{\zeta_{g-}} P(\zeta_g)\mathrm{d}\zeta_g + \int_{\zeta_{g+}}^{+\infty} P(\zeta_g)\mathrm{d}\zeta_g = \frac{1}{2}\mathrm{erfc}\left(\frac{\zeta_{g+}}{\sqrt{2A}}\right) + \frac{1}{2}\mathrm{erfc}\left(-\frac{\zeta_{g-}}{\sqrt{2A}}\right), \quad (17)$$

where $\mathrm{erfc}(x)$ is the complementary error function. While for $-\frac{1}{4\zeta_c} < F_{\mathrm{NL}} < 0$, β becomes

$$\beta = \int_{\zeta_{g-}}^{\zeta_{g+}} P(\zeta_g)\mathrm{d}\zeta_g = \frac{1}{2}\mathrm{erfc}\left(\frac{\zeta_{g-}}{\sqrt{2A}}\right) - \frac{1}{2}\mathrm{erfc}\left(\frac{\zeta_{g+}}{\sqrt{2A}}\right). \quad (18)$$

For $F_{\mathrm{NL}} < -\frac{1}{4\zeta_c}$, the curvature perturbation can never exceed the critical value of forming a PBH. The parameter space in this case is demonstrated in Fig. 3 (the red solid curve). On the other hand, if we require $|\sigma^{(1)}/\sigma^{(0)}| < 1$ to maintain the validity of perturbation theory, this would also place a constraint in the parameter space. The shaded region in Fig. 3 denotes the allowed parameter space which satisfies the perturbativity condition. It can be seen that the two constraints give rise to $-\frac{1}{4} < F_{\mathrm{NL}} \lesssim 35$ for $|\sigma^{(1)}/\sigma^{(0)}| < 1$ and $-\frac{1}{4} < F_{\mathrm{NL}} \lesssim 5$ for $|\sigma^{(1)}/\sigma^{(0)}| < 0.1$.

Second, we switch to the pure G_{NL} case where $F_{\mathrm{NL}} = 0$. In this case, $\zeta(\zeta_g) = \zeta_g + G_{\mathrm{NL}}\zeta_g^3 = \zeta_c$ has at most three real roots. When $G_{\mathrm{NL}} > 0$ or $G_{\mathrm{NL}} < -\frac{4}{27\zeta_c^2}$, there is only one real root, namely,

$$\zeta_1 = -\left(\frac{2^{1/3}}{3}\right)\left[G_{\mathrm{NL}}^2\left(\zeta_c + \sqrt{\zeta_c^2 + \frac{4}{27G_{\mathrm{NL}}}}\right)\right]^{-1/3} + \frac{1}{2^{1/3}G_{\mathrm{NL}}}\left[G_{\mathrm{NL}}^2\left(\zeta_c + \sqrt{\zeta_c^2 + \frac{4}{27G_{\mathrm{NL}}}}\right)\right]^{1/3}, \quad (19)$$

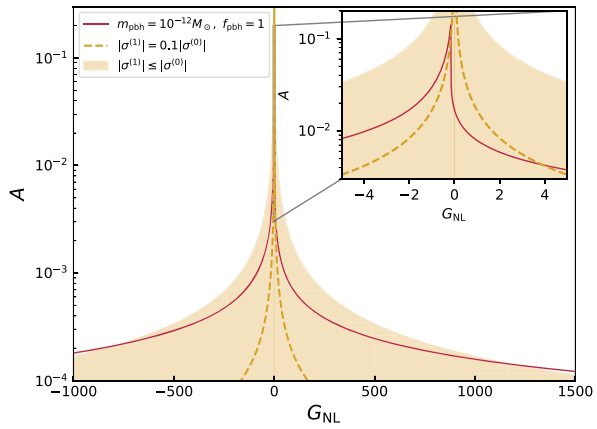

FIG. 4. The allowed parameter space for A and $G_{\rm NL}$ by fixing $F_{\rm NL} = 0$. The shaded region corresponds to $|\sigma^{(1)}/\sigma^{(0)}| \le 1$, and the dashed line corresponds to $|\sigma^{(1)}/\sigma^{(0)}| = 0.1$. If all DM is made up of 10^{-12} $M_\odot$ PBHs, the choice of A and $G_{\rm NL}$ falls on the red curve.

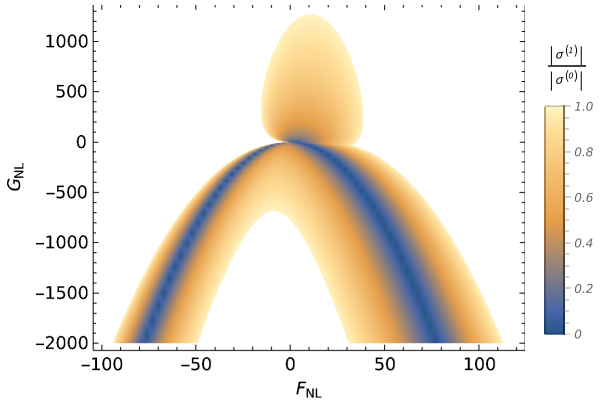

FIG. 5. The parameter space for the non-Gaussian parameters $F_{\rm NL}$ and $G_{\rm NL}$ if 10^{-12} $M_\odot$ PBHs make up all of the DM.

and β is evaluated as

$$\beta = \int_{\zeta_1}^{\infty} P(\zeta_g)\mathrm{d}\zeta_g = \frac{1}{2}\mathrm{erfc}\left(\frac{\zeta_1}{\sqrt{2A}}\right), \tag{20}$$

while for positive $G_{\rm NL}$, it becomes

$$\beta = \int_{-\infty}^{\zeta_1} P(\zeta_g)\mathrm{d}\zeta_g = \frac{1}{2}\mathrm{erfc}\left(\frac{-\zeta_1}{\sqrt{2A}}\right) \tag{21}$$

for $G_{\rm NL} < -\frac{4}{27\zeta_c^2}$. When $-\frac{4}{27\zeta_c^2} < G_{\rm NL} < 0$, there are three real roots $\zeta_1 < 0 < \zeta_2 < \zeta_3$:

$$\begin{aligned}
\zeta_1 &= -\frac{2}{\sqrt{3}(-G_{\rm NL})^{1/2}}\cos(\theta/3), \\
\zeta_2 &= \frac{1}{\sqrt{3}(-G_{\rm NL})^{1/2}}[\cos(\theta/3) - \sqrt{3}\sin(\theta/3)], \\
\zeta_3 &= \frac{1}{\sqrt{3}(-G_{\rm NL})^{1/2}}[\cos(\theta/3) + \sqrt{3}\sin(\theta/3)],
\end{aligned} \tag{22}$$

where we used the notations in [58] such that $\theta = \mathrm{atan}[\frac{(\zeta_t^2-\zeta_c^2)^{1/2}}{\zeta_c}]$ and $\zeta_t \equiv \frac{2}{3\sqrt{3}\sqrt{-G_{\rm NL}}}$. In this case, β takes the form

$$\begin{aligned}
\beta &= \int_{-\infty}^{\zeta_1} P(\zeta_g)\mathrm{d}\zeta_g + \int_{\zeta_2}^{\zeta_3} P(\zeta_g)\mathrm{d}\zeta_g \\
&= \frac{1}{2}\mathrm{erfc}\left(\frac{-\zeta_1}{\sqrt{2A}}\right) + \frac{1}{2}\mathrm{erfc}\left(\frac{\zeta_3}{\sqrt{2A}}\right) - \frac{1}{2}\mathrm{erfc}\left(\frac{\zeta_2}{\sqrt{2A}}\right).
\end{aligned} \tag{23}$$

The parameter space for the pure $G_{\rm NL}$ case is illustrated in Fig. 4. The constraints from the PBH abundance and perturbativity condition lead to $-800 < G_{\rm NL} \lesssim 1200$ for $|\sigma^{(1)}/\sigma^{(0)}| < 1$ and $-0.25 < G_{\rm NL} \lesssim 4$ for $|\sigma^{(1)}/\sigma^{(0)}| < 0.1$.

Finally, for the general case where both $F_{\rm NL}$ and $G_{\rm NL}$ are free, the solution to $\zeta(\zeta_g) = \zeta_c$ is lengthy, and we calculate β numerically. The result is shown in Fig. 5 by fixing $m_{\rm pbh} = 10^{-12}$ $M_\odot$ and $f_{\rm pbh} = 1$. It can be seen that in order to maintain the validity of perturbation theory, one can get constraints on both $F_{\rm NL}$ and $G_{\rm NL}$ for a fixed $m_{\rm pbh}$ and $f_{\rm pbh}$. For $G_{\rm NL} < 0$, the bound of $F_{\rm NL}$ depends on $G_{\rm NL}$, and the lower limit of $G_{\rm NL}$ does not exist, and one can only get a constraint on $F_{\rm NL}$ by considering both the perturbativity condition and PBH abundance. When $G_{\rm NL} > 0$, one can get constraints such that $-20 \lesssim F_{\rm NL} \lesssim 40$ and $G_{\rm NL} \lesssim 1300$ if $|\sigma^{(1)}/\sigma^{(0)}| < 1$, and it turns out that $-1/4 \lesssim F_{\rm NL} \lesssim 4$ and $G_{\rm NL} \lesssim 5$ if $|\sigma^{(1)}/\sigma^{(0)}| < 0.1$.

IV. CONCLUSION AND DISCUSSION

In this paper, we calculate the one-loop correction to the power spectrum of the curvature perturbation with local-type non-Gaussianities. We evaluate the one-loop power spectrum to a general form, and take the δ spectrum and log-normal spectrum as two examples. In order to warrant the validity of perturbation theory, we require that the variance of the one-loop spectrum be much smaller than that of tree level, and we get a perturbativity condition for the non-Gaussian parameters, namely, $|2cAF_{\rm NL}^2 + 6AG_{\rm NL}| \ll 1$. Moreover, the non-Gaussian parameters are tightly constrained if a significant amount of DM is in the form of PBHs.

In general, the non-Gaussian parameters of different orders in the local-type non-Gaussian model should be independent of each other, so it is expected to have no accidental cancellation between the $F_{\rm NL}$ and $G_{\rm NL}$ terms in the one-loop correction. In this sense, each term in the correction should be, respectively, smaller than the tree-level order, and the relations $AF_{\rm NL}^2 \ll \mathcal{O}(1)$ and

$|AG_{\rm NL}| \ll \mathcal{O}(1)$ should hold. On the other hand, the abundance of PBHs would naturally select the non-Gaussian parameters and thus lead to further constraints on the non-Gaussian parameters. For a certain inflation model, the non-Gaussian parameters discussed in this paper could be related to the coefficients in the interaction Hamiltonian above third order. Our work suggests that the consideration of both the perturbativity condition and PBH abundance would place natural constraints on inflation models, which we will leave for future work.

ACKNOWLEDGMENTS

We acknowledge the use of the HPC Cluster of ITP-CAS. This work is supported by the National Key Research and Development Program of China Grant No. 2020YFC2201502, NSFC Grants No. 11975019, No. 11991052, and No. 12047503, Key Research Program of Frontier Sciences, CAS, Grant No. ZDBS-LY-7009, CAS Project for Young Scientists in Basic Research YSBR-006, and the Key Research Program of the Chinese Academy of Sciences Grant No. XDPB15.

[1] Y. B. Zel'dovich and I. D. Novikov, Sov. Astron. **10**, 602 (1967), https://adsabs.harvard.edu/full/1967SvA....10..602Z.
[2] S. Hawking, Mon. Not. R. Astron. Soc. **152**, 75 (1971).
[3] B. J. Carr and S. W. Hawking, Mon. Not. R. Astron. Soc. **168**, 399 (1974).
[4] B. J. Carr, Astrophys. J. **201**, 1 (1975).
[5] M. Sasaki, T. Suyama, T. Tanaka, and S. Yokoyama, Phys. Rev. Lett. **117**, 061101 (2016); **121**, 059901(E) (2018).
[6] Z.-C. Chen and Q.-G. Huang, Astrophys. J. **864**, 61 (2018).
[7] M. Raidal, C. Spethmann, V. Vaskonen, and H. Veermäe, J. Cosmol. Astropart. Phys. 02 (2019) 018.
[8] V. De Luca, G. Franciolini, P. Pani, and A. Riotto, J. Cosmol. Astropart. Phys. 06 (2020) 044.
[9] A. Hall, A. D. Gow, and C. T. Byrnes, Phys. Rev. D **102**, 123524 (2020).
[10] S. Bhagwat, V. De Luca, G. Franciolini, P. Pani, and A. Riotto, J. Cosmol. Astropart. Phys. 01 (2021) 037.
[11] G. Hütsi, M. Raidal, V. Vaskonen, and H. Veermäe, J. Cosmol. Astropart. Phys. 03 (2021) 068.
[12] K. W. K. Wong, G. Franciolini, V. De Luca, V. Baibhav, E. Berti, P. Pani, and A. Riotto, Phys. Rev. D **103**, 023026 (2021).
[13] V. De Luca, G. Franciolini, P. Pani, and A. Riotto, J. Cosmol. Astropart. Phys. 05 (2021) 003.
[14] G. Franciolini, V. Baibhav, V. De Luca, K. K. Y. Ng, K. W. K. Wong, E. Berti, P. Pani, A. Riotto, and S. Vitale, Phys. Rev. D **105**, 083526 (2022).
[15] Z.-C. Chen, C. Yuan, and Q.-G. Huang, Phys. Lett. B **829**, 137040 (2022).
[16] B. J. Carr, K. Kohri, Y. Sendouda, and J. Yokoyama, Phys. Rev. D **81**, 104019 (2010).
[17] L. Chen, Q.-G. Huang, and K. Wang, J. Cosmol. Astropart. Phys. 12 (2016) 044.
[18] Y. Ali-Haïmoud and M. Kamionkowski, Phys. Rev. D **95**, 043534 (2017).
[19] D. Aloni, K. Blum, and R. Flauger, J. Cosmol. Astropart. Phys. 05 (2017) 017.
[20] B. Horowitz, arXiv:1612.07264.
[21] S. Bird, I. Cholis, J. B. Muñoz, Y. Ali-Haïmoud, M. Kamionkowski, E. D. Kovetz, A. Raccanelli, and A. G. Riess, Phys. Rev. Lett. **116**, 201301 (2016).
[22] J. García-Bellido, J. Phys. Conf. Ser. **840**, 012032 (2017).
[23] M. Sasaki, T. Suyama, T. Tanaka, and S. Yokoyama, Classical Quantum Gravity **35**, 063001 (2018).
[24] L. Barack *et al.*, Classical Quantum Gravity **36**, 143001 (2019).
[25] Z.-C. Chen, F. Huang, and Q.-G. Huang, Astrophys. J. **871**, 97 (2019).
[26] Z.-C. Chen and Q.-G. Huang, J. Cosmol. Astropart. Phys. 08 (2020) 039.
[27] A. Barnacka, J.-F. Glicenstein, and R. Moderski, Phys. Rev. D **86**, 043001 (2012).
[28] P. W. Graham, S. Rajendran, and J. Varela, Phys. Rev. D **92**, 063007 (2015).
[29] H. Niikura *et al.*, Nat. Astron. **3**, 524 (2019).
[30] K. Griest, A. M. Cieplak, and M. J. Lehner, Phys. Rev. Lett. **111**, 181302 (2013).
[31] P. Tisserand *et al.* (EROS-2 Collaboration), Astron. Astrophys. **469**, 387 (2007).
[32] T. D. Brandt, Astrophys. J. Lett. **824**, L31 (2016).
[33] D. Gaggero, G. Bertone, F. Calore, R. M. T. Connors, M. Lovell, S. Markoff, and E. Storm, Phys. Rev. Lett. **118**, 241101 (2017).
[34] H. Niikura, M. Takada, S. Yokoyama, T. Sumi, and S. Masaki, Phys. Rev. D **99**, 083503 (2019).
[35] S. Wang, Y.-F. Wang, Q.-G. Huang, and T. G. F. Li, Phys. Rev. Lett. **120**, 191102 (2018).
[36] B. P. Abbott *et al.* (LIGO Scientific and Virgo Collaborations), Phys. Rev. Lett. **121**, 231103 (2018).
[37] R. Magee, A.-S. Deutsch, P. McClincy, C. Hanna, C. Horst, D. Meacher, C. Messick, S. Shandera, and M. Wade, Phys. Rev. D **98**, 103024 (2018).
[38] P. Montero-Camacho, X. Fang, G. Vasquez, M. Silva, and C. M. Hirata, J. Cosmol. Astropart. Phys. 08 (2019) 031.
[39] R. Laha, Phys. Rev. Lett. **123**, 251101 (2019).
[40] Z.-C. Chen, C. Yuan, and Q.-G. Huang, Phys. Rev. Lett. **124**, 251101 (2020).
[41] G. Defillon, E. Granet, P. Tinyakov, and M. H. Tytgat, Phys. Rev. D **90**, 103522 (2014).
[42] A. Katz, J. Kopp, S. Sibiryakov, and W. Xue, J. Cosmol. Astropart. Phys. 12 (2018) 005.

[43] B. Carr, K. Kohri, Y. Sendouda, and J. Yokoyama, Rep. Prog. Phys. **84**, 116902 (2021).
[44] B. Carr and F. Kuhnel, Annu. Rev. Nucl. Part. Sci. **70**, 355 (2020).
[45] Y. Akrami *et al.* (Planck Collaboration), Astron. Astrophys. **641**, A10 (2020).
[46] G. Franciolini, A. Kehagias, S. Matarrese, and A. Riotto, J. Cosmol. Astropart. Phys. 03 (2018) 016.
[47] M. Biagetti, G. Franciolini, A. Kehagias, and A. Riotto, J. Cosmol. Astropart. Phys. 07 (2018) 032.
[48] V. Atal and C. Germani, Phys. Dark Universe **24**, 100275 (2019).
[49] S. Passaglia, W. Hu, and H. Motohashi, Phys. Rev. D **99**, 043536 (2019).
[50] V. Atal, J. Garriga, and A. Marcos-Caballero, J. Cosmol. Astropart. Phys. 09 (2019) 073.
[51] V. Atal, J. Cid, A. Escrivà, and J. Garriga, J. Cosmol. Astropart. Phys. 05 (2020) 022.
[52] M. Taoso and A. Urbano, J. Cosmol. Astropart. Phys. 08 (2021) 016.
[53] M. Biagetti, V. De Luca, G. Franciolini, A. Kehagias, and A. Riotto, Phys. Lett. B **820**, 136602 (2021).
[54] M. W. Davies, P. Carrilho, and D. J. Mulryne, J. Cosmol. Astropart. Phys. 06 (2022) 019.
[55] J. M. Maldacena, J. High Energy Phys. 05 (2003) 013.
[56] M. H. Namjoo, H. Firouzjahi, and M. Sasaki, Europhys. Lett. **101**, 39001 (2013).
[57] J. Kristiano and J. Yokoyama, Phys. Rev. Lett. **128**, 061301 (2022).
[58] C. T. Byrnes, E. J. Copeland, and A. M. Green, Phys. Rev. D **86**, 043512 (2012).
[59] K. Kohri and T. Terada, Phys. Rev. D **97**, 123532 (2018).
[60] N. Bartolo, V. De Luca, G. Franciolini, M. Peloso, D. Racco, and A. Riotto, Phys. Rev. D **99**, 103521 (2019).
[61] N. Bartolo, V. De Luca, G. Franciolini, A. Lewis, M. Peloso, and A. Riotto, Phys. Rev. Lett. **122**, 211301 (2019).
[62] C. Yuan, Z.-C. Chen, and Q.-G. Huang, Phys. Rev. D **100**, 081301 (2019).
[63] I. Musco, J. C. Miller, and L. Rezzolla, Classical Quantum Gravity **22**, 1405 (2005).
[64] I. Musco, J. C. Miller, and A. G. Polnarev, Classical Quantum Gravity **26**, 235001 (2009).
[65] I. Musco and J. C. Miller, Classical Quantum Gravity **30**, 145009 (2013).
[66] T. Harada, C.-M. Yoo, and K. Kohri, Phys. Rev. D **88**, 084051 (2013); **89**, 029903(E) (2014).
[67] V. De Luca and A. Riotto, Phys. Lett. B **828**, 137035 (2022).
[68] T. Nakama, J. Silk, and M. Kamionkowski, Phys. Rev. D **95**, 043511 (2017).